

# We are IntechOpen, the world's leading publisher of Open Access books Built by scientists, for scientists

6,900

Open access books available

186,000

International authors and editors

200M

Downloads

Our authors are among the

154

Countries delivered to

TOP 1%

most cited scientists

12.2%

Contributors from top 500 universities



WEB OF SCIENCE™

Selection of our books indexed in the Book Citation Index  
in Web of Science™ Core Collection (BKCI)

Interested in publishing with us?  
Contact [book.department@intechopen.com](mailto:book.department@intechopen.com)

Numbers displayed above are based on latest data collected.  
For more information visit [www.intechopen.com](http://www.intechopen.com)



# Titanium Dioxide and Its Applications in Mechanical, Electrical, Optical, and Biomedical Fields

*Rajib Das, Vibhav Ambardekar  
and Partha Pratim Bandyopadhyay*

## Abstract

Titanium dioxide ( $\text{TiO}_2$ ), owing to its non-toxicity, chemical stability, and low cost, is one of the most valuable ceramic materials.  $\text{TiO}_2$  derived coatings not only act like a ceramic protective shield for the metallic substrate but also provide cathodic protection to the metals against the corrosive solution under Ultraviolet (UV) illumination. Being biocompatible,  $\text{TiO}_2$  coatings are widely used as an implant material. The acid treatment of  $\text{TiO}_2$  promotes the attachment of cells and bone tissue integration with the implant. In this chapter, the applications of  $\text{TiO}_2$  as a corrosion inhibitor and bioactive material are briefly discussed. The semiconducting nature and high refractive index of  $\text{TiO}_2$  conferred UV shielding properties, allowing it to absorb or reflect UV rays. Several studies showed that a high ultraviolet protection factor (UPF) was achieved by incorporating  $\text{TiO}_2$  in the sunscreens (to protect the human skin) and textile fibers (to minimize its photochemical degradation). The rutile phase of  $\text{TiO}_2$  offers high whiteness, and opacity owing to its tendency to scatter light. These properties enable  $\text{TiO}_2$  to be used as a pigment a brief review of which is also addressed in this chapter. Since  $\text{TiO}_2$  exhibits high hardness and fracture toughness, the wear rate of composite is considerably reduced by adding  $\text{TiO}_2$ . On interacting with gases like hydrogen at elevated temperatures, the electrical resistance of  $\text{TiO}_2$  changes to some different value. The change in resistance can be utilized in detecting various gases that enables  $\text{TiO}_2$  to be used as a gas sensor for monitoring different gases. This chapter attempts to provide a comprehensive review of applications of  $\text{TiO}_2$  as an anti-corrosion, wear-resistant material in the mechanical field, a UV absorber, pigment in the optical sector, a bioactive material in the biomedical field, and a gas sensor in the electrical domain.

**Keywords:** Titanium dioxide, properties, applications, corrosion resistance, wear resistance, UV absorber, biomaterials, gas sensors

## 1. Introduction

Titanium dioxide ( $\text{TiO}_2$ ) is a naturally occurring oxide of titanium. It is also referred to as titanium (IV) oxide or titania.  $\text{TiO}_2$  is a cheap and widely available white oxide

ceramic having a molecular mass of 79.86 g/mol, a density of 3.9–4.2 g/cm<sup>3</sup>, a refractive index in the range of 2.5–2.75, and Mohs hardness of 5.5–7 [1]. It occurs in three crystalline forms: rutile, anatase, and brookite. Both rutile and anatase have a tetragonal structure, whereas brookite has an orthorhombic structure. In industrial applications, only anatase and rutile phases of TiO<sub>2</sub> are used [1]. TiO<sub>2</sub> also serves as a semiconductor, with a band gap of 3.2 eV for anatase and 3.0 eV for rutile. TiO<sub>2</sub> is non-toxic, chemically as well as photo-chemically stable, non-flammable, and biocompatible [2]. TiO<sub>2</sub> is often deposited as thin films or thick film coatings to impart anti-wear and corrosion-resistant properties [3]. It is also used in gas sensing and biomedical applications. Because of its UV absorption ability, TiO<sub>2</sub> has also been used in sunscreens. TiO<sub>2</sub> is also suitable to be used as white pigments. In the past few decades, research activities on nanomaterials have grown rapidly since materials in nano size exhibit completely different properties as compared to their bulk properties. As a result, TiO<sub>2</sub> is one of the most extensively used nano-size materials and is found to be useful in a wide range of applications [4].

## 2. Applications of titanium dioxide

Owing to its appealing electrical, optical, and mechanical attributes, TiO<sub>2</sub> coating is commonly utilized for gas detecting, wear-resistant, UV shielding, and corrosion-resistant applications. It is also used as a pigment in paints, coatings, cosmetics, plastics, etc. TiO<sub>2</sub> also plays an important role in the fabrication of medical implants. **Figure 1** depicts the applications of TiO<sub>2</sub> in various sectors. These applications of TiO<sub>2</sub> are discussed in the subsequent sections.

### 2.1 Corrosion resistance

From a technical standpoint, it is crucial to keep metals free of corrosion [5]. One of the most effective techniques to protect metals from corrosion is to apply a protective layer to the metal's surface [6, 7]. Organic coatings are often used in the industry for such purposes [8]. In addition to organic coatings, ceramic coatings have gained popularity in this field due to their superior resistance to oxidation and corrosion in high-temperature or corrosive environments [9–12]. TiO<sub>2</sub> coating is an example of a ceramic coating that is commonly used as a protective layer [13].

There are different ways of depositing TiO<sub>2</sub> films over the metallic surface. Researchers have attempted a variety of methods of depositing TiO<sub>2</sub> on the substrate to investigate its ability in protecting the substrate from corrosion. Masalski et al. [14] proposed plasma assisted chemical vapor deposition (PACVD) as one such approach to obtain TiO<sub>2</sub> films on the 316 steel. The un-coated specimen showed the pitting nucleation (breakdown) at 0.2–0.3 V. However, pitting corrosion was not observed for TiO<sub>2</sub>-coated specimen even at 3 V. Furthermore, the current densities of TiO<sub>2</sub>-coated specimen were found to be significantly lower than those of the uncoated sample. This demonstrated the efficacy of TiO<sub>2</sub> as a corrosion inhibitor.

Ceramic coatings are often deposited using plasma spraying [15]. However, the metal substrate and bond coat are exposed to corrosion owing to the existence of pores within the coating [16]. Yan et al. [17] tested the corrosion resistance of alumina (Al<sub>2</sub>O<sub>3</sub>) composite coating in dilute hydrochloric acid (HCl) solution. They reported that the connectivity of pores in the composite coating was lowered by adding 13 wt. % TiO<sub>2</sub> to Al<sub>2</sub>O<sub>3</sub>. As a result, the composite coating exhibited better resistance to corrosion than the Al<sub>2</sub>O<sub>3</sub> coating without any dopants.

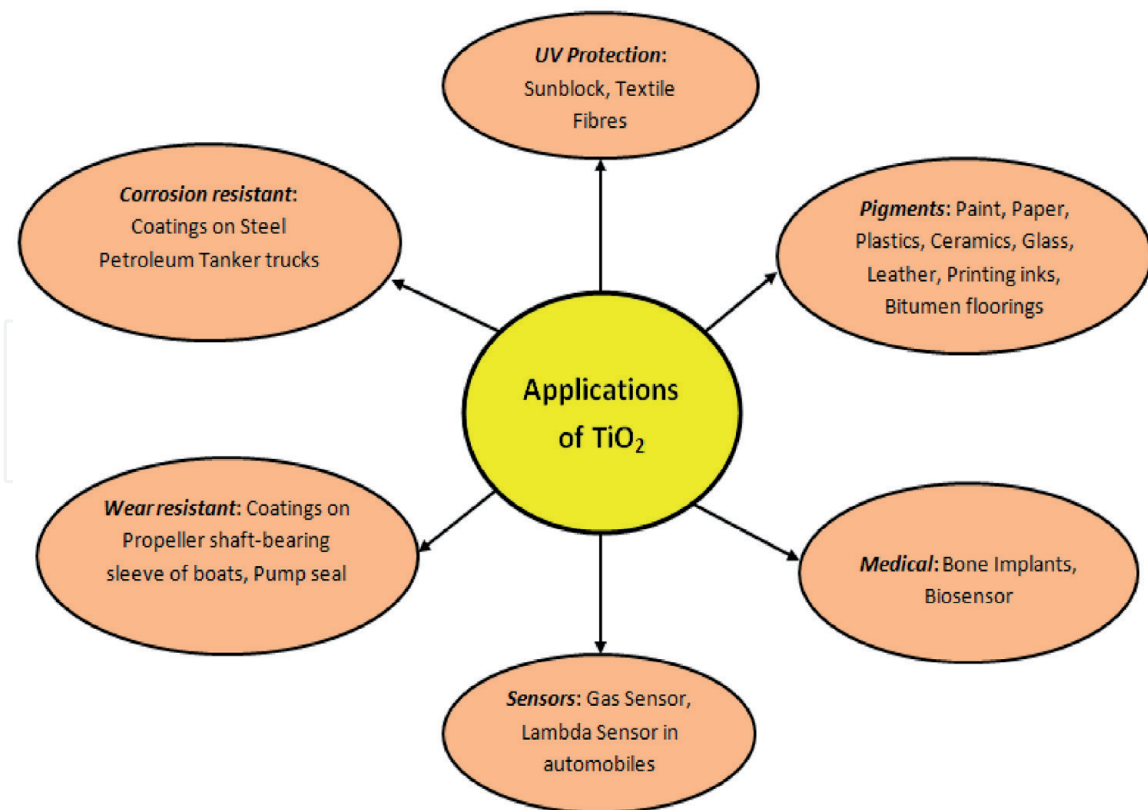


**Figure 1.**  
*Some applications of TiO<sub>2</sub> in different domains.*

Several researchers tested the potential of TiO<sub>2</sub> thin films under UV light. TiO<sub>2</sub> is an n-type semiconductor, upon exposed to UV illumination, the electrons flow towards the metal through the conduction band of TiO<sub>2</sub>. Consequently, the metal's potential will be lower than that required for oxidation. If this occurs, metals can be protected from corrosion. Moreover, TiO<sub>2</sub> film is not decomposed and can act as a non-sacrificial anode. Copper and stainless steel could be cathodically protected using TiO<sub>2</sub> film under UV illumination [18]. Ohko et al. [18] prepared TiO<sub>2</sub> films on 304 stainless steel (SUS 304) using the spray pyrolysis technique. It was subjected to a corrosion test in a sodium chloride (NaCl) solution with a pH higher than 3. When irradiated with UV light of intensity 10 mW/cm<sup>2</sup>, they observed that the photopotential of TiO<sub>2</sub> coated specimen was lower than that of uncoated SUS 304. It showed that under illumination, a photo-electrochemical property was exhibited by TiO<sub>2</sub> that rendered cathodic protection to the metals [19].

Titanium coating can shield the aluminum alloy from pitting corrosion. The thermal oxidation of this coating can further improve the anti-corrosion property of the substrate. This is owing to the formation of a dense TiO<sub>2</sub> layer of rutile phase on the surface of the titanium coating during thermal oxidation. This formation of the TiO<sub>2</sub> layer is responsible for the reduction in corrosion rates. The oxidation temperature and time are the two factors that have a direct impact on the degree of improvement [20].

Shen et al. [19] studied the corrosion protection behavior of nano TiO<sub>2</sub> coatings on 316 L stainless steel in both dim and UV illumination conditions. A sol-gel method was used to create TiO<sub>2</sub> nanoparticle coating, which was subsequently exposed to hydrothermal treatment. When tested in 0.5 molL<sup>-1</sup> NaCl solution in a dark environment, the coating exhibited excellent resistance to corrosion as it acted like a ceramic protective shield on the metal's surface. This was corroborated by the fact that in comparison to uncoated steel, the corrosion current density was

decreased by three orders of magnitude and the corrosion resistance was enhanced by more than a hundredfold for TiO<sub>2</sub> nanoparticle coated stainless steel. However, the electrons generated under UV illumination offered cathodic protection to the stainless steel substrate. Mahmoud et al. [21] also reported that the TiO<sub>2</sub> layer deposited on weathering steel displayed higher anti-corrosion properties than the bare steel in NaCl aqueous solution, under UV light.

Shan et al. [22] employed the atomic layer deposition (ALD) technique to deposit a thin TiO<sub>2</sub> film of thickness 50 nm onto stainless steel. X-ray diffraction (XRD) results indicated the amorphous structure of TiO<sub>2</sub>. When steel was evaluated for corrosion, the corrosion potential increased from -0.96 eV to -0.63 eV on applying TiO<sub>2</sub> coating. In addition, the corrosion current density was reduced from  $7.0 \times 10^{-7}$  A/cm<sup>2</sup> for uncoated steel to  $6.3 \times 10^{-8}$  A/cm<sup>2</sup> for coated steel. This implied that the TiO<sub>2</sub> film was effective in shielding the stainless steel substrate against the corrosive agents.

Anti-corrosion coatings are usually made of epoxy resins. However, micro-pores are created during their curing process. The corrosive medium can easily penetrate the epoxy coating through these micro-pores, making the substrate highly susceptible to corrosion. To improve the anti-corrosion characteristics of epoxy coatings, Yu et al. [23] developed hybrid modified graphene oxide (GO) sheets by incorporating nano-TiO<sub>2</sub> on the surface of graphene oxide using 3-aminopropyltriethoxysilane. The interlayer gap of the sheets was observed to rise as a result of this. Owing to this greater interlayer spacing, the TiO<sub>2</sub>-GO hybrids were easily exfoliated and disseminated in the epoxy coating. The electrochemical impedance spectroscopy (EIS) test revealed that adding merely 2 wt. % of TiO<sub>2</sub>-GO hybrid to epoxy resulted in a tremendous improvement in the corrosion resistance. This was attributed to the sheet-like structure of hybrid which behaved as an additional barrier layer, preventing the corrosive liquid medium from accessing the micro-pores. Excellent plugging of micro-pores by this hybrid led to an improved anti-corrosion performance of such coating.

Khalajabadi et al. [24] studied the effect of adding TiO<sub>2</sub> nanopowders on the anticorrosion performance of magnesium/hydroxyapatite (Mg/HA)-based nanocomposite for medical applications. TiO<sub>2</sub> doped nanocomposite was synthesized by the milling-pressing-sintering technique. They reported that the addition of 15 wt. % TiO<sub>2</sub> nanopowders and a drop in HA amount to 5 wt. %, resulted in a decrease in the number of pores and HA agglomeration. Moreover, the wettability of the samples after sintering was reduced owing to the formation of magnesium titanate (MgTiO<sub>3</sub>) nanoflakes. This obstructed the electrolyte from penetrating the nanocomposite. The corrosion current of the composite without TiO<sub>2</sub> was 285.3  $\mu$ A/cm<sup>2</sup>, which drastically reduced to 4.8  $\mu$ A/cm<sup>2</sup> for nanocomposite containing TiO<sub>2</sub>. Similarly, the polarization resistance of Mg/HA increased dramatically from 0.25 k $\Omega$  cm<sup>2</sup> to 11.86 k $\Omega$  cm<sup>2</sup> with the incorporation of TiO<sub>2</sub>. On doping TiO<sub>2</sub>, the corrosion rate of composite coating reduced remarkably from 4.28 mm/yr. to 0.1 mm/yr. These findings suggested that the corrosion resistance of Mg/HA-based nanocomposite could be improved significantly by adding TiO<sub>2</sub> nanopowders. Similarly, the addition of TiO<sub>2</sub> nanoparticles in the nickel-tungsten (Ni-W) alloy matrix enhanced its anti-corrosion characteristics as compared to Ni-W alloy [25]. Poorraeisi et al. [26] also reported that the incorporation of zirconium oxide-titanium oxide (ZrO<sub>2</sub>-TiO<sub>2</sub>) in hydroxyapatite coating showed better resistance to corrosion than the coating without ZrO<sub>2</sub>-TiO<sub>2</sub> reinforcement.

Epoxy coatings can be applied on steel petroleum tanker trucks to protect them from corrosion as they provide a physical barrier layer and offer excellent chemical stability [27]. Several reports have suggested the use of nanoparticles in epoxy coatings to further enhance its anticorrosion characteristics. Nanoparticles

possess excellent surface properties and can block pores, cavities, and channels in the coating. As a result, they serve as a buffer against the electrolyte, preventing the corrosive solution from diffusing into the coating. TiO<sub>2</sub>/epoxy nanocomposites significantly elevate the corrosion resistance of epoxy resins. The anti-corrosion behavior of poly-dimethylaminosiloxane (PDMAS)/TiO<sub>2</sub> epoxy hybrid nanocomposite coating and traditional epoxy coating were tested using salt spray accelerated corrosion test by Fadl et al. [27]. The scanning electron microscope (SEM) and energy dispersive X-ray spectroscopy (EDS) analysis as well as the weight loss study confirmed that the hybrid nanocomposite coating was superior to conventional epoxy coating in terms of anti-corrosion properties.

Krishna et al. [28] developed TiO<sub>2</sub> film over commercially pure titanium by thermal oxidation. In this report, when thermal air oxidation was carried out at a temperature less than 400°C for 1 hour, the corrosion resistance of the TiO<sub>2</sub> film increased with the increase in the film thickness. They discovered that the rutile phase of TiO<sub>2</sub> films exhibited better anti-corrosion properties than the amorphous phase.

A thin layer of ceramic coating on aluminum alloy is effective in protecting it from corrosion. To achieve long-term protection from corrosion, Merisalu et al. [29] deposited two different layers of coating on aluminum alloy. Initially, a thin film of nanoporous aluminum oxide base layer was deposited on the substrate using a special anodizing process. The nano-sized pores present in this aluminum oxide layer were then sealed by depositing chemically resistant aluminum oxide/titanium oxide (Al<sub>2</sub>O<sub>3</sub>/TiO<sub>2</sub>) nanolaminates using ALD. The Al<sub>2</sub>O<sub>3</sub>/TiO<sub>2</sub> nanolaminates not only transformed the base layer into a nanocomposite but also covered the entire surface of the base layer to form the top-most layer of coatings. The samples underwent corrosion tests by immersing them in a salt solution for a longer duration. The tests revealed that the top layer of Al<sub>2</sub>O<sub>3</sub>/TiO<sub>2</sub> nanolaminates significantly improved the corrosion resistance of coating by acting as an ion barrier. This coating was able to withstand the salt solution for 298 days. Atomic layer deposition of Al<sub>2</sub>O<sub>3</sub> and TiO<sub>2</sub> nanolaminates as a corrosion inhibitor was also reported in other papers [30, 31].

Biomedical magnesium alloys such as WE43 Mg alloy must exhibit excellent resistance to corrosion in a physiological environment. To protect it from corrosion by simulated body fluid (SBF), Li et al. [32] electrodeposited nanocrystalline zinc (Zn) coating on WE43 Mg alloy. This coating was further chemically treated to form a Titanium oxide-Zinc phosphate layer. In SBF, this composite coating displayed a much lower corrosion current density of  $4.1 \pm 0.8 \mu\text{A}/\text{cm}^2$  and a much larger resistance of  $4.28 \times 10^3 \Omega \text{ cm}^2$  than uncoated WE and WE alloy with only Zn coating. WE alloy with Zn coating showed poor corrosion resistance because of the establishment of galvanic couples between the Zn coating and WE43 Mg alloy substrate.

Nanomaterials offer a larger surface area than conventional materials which can considerably influence the anticorrosion performance of nano-coatings. Chen et al. [33] observed that the average corrosion potential of bare titanium alloy (Ti-6Al-4 V) in the presence of NaCl solution was 0.316 V which was reduced to 0.07 V for TiO<sub>2</sub> nanoparticle coated titanium alloy.

## 2.2 UV protection

Ultraviolet (UV) rays coming from the sun are the radiations having a wavelength in the range of 200–400 nm. UV rays are generally known to have detrimental effects on the skin health of the human body. These UV rays can be categorized into three groups: Ultraviolet C (wavelengths range of 200 to 290 nm) denoted as UVC, Ultraviolet B (wavelengths range of 290–320 nm) denoted as

UVB, and Ultraviolet A (wavelengths range of 320–400 nm) denoted as UVA. UVC is blocked by the atmosphere and cannot reach the earth. UVB causes sunburn, however, it is absorbed by the glass and therefore rooms with glass windows can block the UVB rays from entering the room. UVA, on the other hand, can transmit through the glass and inflict serious skin damage, possibly leading to skin cancer [34]. Sunscreen is often applied to protect the skin from these harmful rays. There are two types of sunblock available. One is an organic sunblock, which absorbs UV rays and converts them into heat, and the other one is inorganic.  $\text{TiO}_2$  and  $\text{ZnO}$  are examples of inorganic sunblock [35].  $\text{TiO}_2$  provides exceptional blocking against UVA and UVB radiation owing to its chemical and physical properties. However, its UV protection mechanisms are still being studied [36].  $\text{TiO}_2$  is a semiconductor, and its UV absorption ability can be understood from the band theory of solids.  $\text{TiO}_2$  is capable of absorbing UV rays due to the formation, mobility, and separation of photo-generated electrons and holes [37, 38]. Some researchers believe that because of the high refractive index of  $\text{TiO}_2$ , the UV rays are reflected and/or scattered, resulting in high UV-shielding properties. Apart from protecting the skin from harmful UV rays, the UV-blocking properties of  $\text{TiO}_2$  can also benefit the textile industry by minimizing the photochemical degradation and color fading of textile fibers after prolonged UV exposure.

There are several research publications available that indicate the UV protection of textile substrates by  $\text{TiO}_2$  [39–44]. The UV resistance performance is measured by calculating the ultraviolet protection factor (UPF) for UVA and UVB. Higher UPF values in the range of 40–50 or above 50 indicate lower transmission of UV rays. A UPF value of 50 indicates that only 1/50 (or 2%) of UV radiation transmits through the textile material and reaches the skin. UV absorption spectra can also be used to assess UV resistance. With a UPF value of 10, an untreated cotton fabric displayed insufficient UV protection, whereas when it was treated with  $\text{TiO}_2$  nanoparticles, the cotton material offered a maximum UPF value of 50 [45].

Engineering polymer such as polyetheretherketone (PEEK) suffers from chemical degradation when exposed to UV radiation. This also results in its discolouration and loss of mechanical properties such as ductility. To boost the UV resistance, Bragaglia et al. [46] incorporated submicron size  $\text{TiO}_2$  as fillers in the PEEK matrix to form PEEK- $\text{TiO}_2$  composites. The volume fraction of  $\text{TiO}_2$  was varied from 0 to 5%. The UV-thermal aging of samples was conducted for 8 hours at a temperature of 70°C using 351 nm peaked UVA radiation with an intensity of 0.77 W/m<sup>2</sup>. Following that, the samples were exposed to the humid condition of 100% RH at 50°C for 4 hours. The cycles were repeated for 30 days. The UV aging test revealed that the composite containing 5 vol.% of  $\text{TiO}_2$  was effective in retarding the photo-degradation of the PEEK polymer because of the UV-blocking action of  $\text{TiO}_2$ . It was also reported that the tensile strength and ductility of the PEEK- 5 vol. %  $\text{TiO}_2$  composite remain unaltered even after exposure to UV rays.

Li et al. [47] prepared  $\text{TiO}_2$  coated polyester (PET) to enhance its UV resistance and anti-aging characteristics. To carry out the UV aging test, the specimens (both coated and uncoated fabrics) were exposed to UV irradiation of intensity 0.89 W/m<sup>2</sup>/nm for 60°C for a specific period. The effect of UV irradiation on the breaking strength of the fabrics was also tested. The  $\text{TiO}_2$ -coated PET displayed excellent UV resistance as its UPF was reported to be 130 in contrast to 34 for uncoated PET. After 100 hours of UV exposure, the strength of uncoated PET was reduced by 44% in warp direction whereas, for coated PET, the strength was reduced by 35.6%.

Torbati et al. [34] compared the UV resistance of base sunscreen cream to one containing 0.5% w/w  $\text{TiO}_2$  nanoparticle. The sun protection factor (SPF) against UV radiation was measured for both the creams. The cream containing  $\text{TiO}_2$  showed

a significantly high SPF rating compared to the base cream, indicating superior UV protection by the TiO<sub>2</sub> doped cream.

Natural rubber (NR) is prone to photo-oxidation when exposed to UV light. The double bonds in NR chains are attacked by the UV rays which lead to changes in the mechanical properties. Seentrakoon et al. [48] prepared nanoparticles of rutile TiO<sub>2</sub> (n-TiO<sub>2</sub>) from micron-sized rutile TiO<sub>2</sub> (micro-TiO<sub>2</sub>) through ultrasonication. This n-TiO<sub>2</sub> was mixed with natural rubber to explore its UV shielding properties. The UV blocking performance of the n-TiO<sub>2</sub>/NR composite was compared with the unfilled NR. The UV resistance of the prepared nanocomposites was tested using accelerated weathering tester equipped with a UVA 340 nm fluorescent lamp of light intensity 0.63 W/m<sup>2</sup>/nm. The test was conducted at a temperature of 50°C for 24 hours. The extent of retention of the mechanical properties after UV irradiation was also assessed for all the samples. The unfilled NR displayed a strong carbonyl peak after exposure to UV light. This indicated a high degree of degradation of NR by UV rays. On the other hand, the carbonyl peak intensity was significantly reduced with the addition of n-TiO<sub>2</sub>. This demonstrated that an effective UV photodegradation prevention was achieved by the incorporation of n-TiO<sub>2</sub>. The n-TiO<sub>2</sub> doped NR composite was reported to be more effective in shielding UV rays than the unfilled NR and NR composite containing micron-sized rutile TiO<sub>2</sub> (micro TiO<sub>2</sub>/NR). The mechanical strength testing of these specimens revealed that the percentage retention of tensile strength and elongation at break after exposure to UV rays for NR was 51.2%, and 84%, respectively which climbed to 90.6%, and 92.9%, respectively for n-TiO<sub>2</sub>/NR. The characteristics of micro-TiO<sub>2</sub>/NR were intermediate between those of unfilled NR and n-TiO<sub>2</sub>/NR. The considerable increment in the percentage retention of mechanical properties confirmed that n-TiO<sub>2</sub>/NR composite provided better UV protection and prevented the NR from the negative impact of UV. The high UV shielding performance of n-TiO<sub>2</sub> than micro-TiO<sub>2</sub> was attributed to the high surface area per particle size of n-TiO<sub>2</sub> which significantly boosted the UV shielding property.

Reinosa et al. [49] formulated a sunscreen using a combination of nano zinc oxide (ZnO) and micro-TiO<sub>2</sub> composite. They claimed that this product not only provided a greater SPF but was also capable of reducing nanoparticle diffusion into the skin of the human body.

Sun et al. [50] investigated the influence of TiO<sub>2</sub> layer thickness on the solar energy conversion efficiency and illumination stability of the polymer solar cell. TiO<sub>2</sub> layers were formed by the spray pyrolysis technique. By functioning as a UV blocker, the photodegradation of the organic solar cell was decreased with an increase in the TiO<sub>2</sub> layer thickness. The thick TiO<sub>2</sub> layer, on the other hand, restricted the amount of light falling on the solar cell and lowered its performance. Considering both the positive and the negative effects, it was stated that the TiO<sub>2</sub> layer of 100 nm thickness was the optimum thickness for this solar cell.

The morphology and the content of TiO<sub>2</sub> largely influence its UV-shielding properties. The increment in UPF value with the addition of TiO<sub>2</sub> has been documented in numerous studies [41, 43]. TiO<sub>2</sub> is also doped with other UV absorbing materials to enhance the UV blocking properties. Noble metals such as gold and silver are also effective UV absorbers and combining TiO<sub>2</sub> with such noble metals improved the UV protection of cotton fabrics [39, 41, 44].

Liang et al. [42] prepared a composite with natural pigment melanin and TiO<sub>2</sub>. Melanin protects the living cell from UV radiation. Wool fabrics were treated with such organic-inorganic composite to impart UV protection characteristics. They found that when untreated wool cloth with a UPF of 25 was treated with pure-melanin, pure-TiO<sub>2</sub>, and melanin/TiO<sub>2</sub> composite, the UPF value increased to 40, 83.9, and 112.6, respectively. Similarly, Li et al. [47] reported that the TiO<sub>2</sub>-coated

polyester fabric with a UPF of 130 rose to 135 when coated with a mixture of TiO<sub>2</sub> and benzotriazole (an organic UV absorber).

### 2.3 Bioactive materials

Medical implants are structures that provide support or can be a substitute for injured biological tissue. A biocompatible medical implant encourages a healthy relationship between the implant and the surrounding tissue. A medical implant must not release any harmful substances into the body. It must not trigger an inflammatory response as well. Some of the examples of implants include artificial hearts, bone implants, dental structures, etc. Titanium (Ti) and its alloys such as nitinol (TiNi) possess desirable mechanical properties and biocompatibility, making them ideal for use as bone implants [51]. But Ti-based metallic materials cannot form chemical bonds with bone tissues. Hence, the formation of new bone becomes complicated during the initial stages of implantation, resulting in low bioactivity and a reduction in the service time of the implant. Furthermore, the release of dangerous metallic ions from the titanium alloy in the biological environment may result in toxic reactions [52]. Therefore, the surface of the implant needs to be modified to encourage the development and growth of the bone tissue on the implants, as well as to enhance the implant's integration with the bone tissues.

Because of its superior biocompatibility and anti-corrosion properties, TiO<sub>2</sub> coatings on the surface of implants have gotten a lot of attention in the biomedical industry [53]. There are various methods of depositing TiO<sub>2</sub> coating which include laser ablation, dip coating, sol-gel process, heat treatment, electrochemical methods [54], sputtering, thermal spraying, etc. [55]. TiO<sub>2</sub> films fabricated by anodic oxidation process in sulfuric acid under potentiostatic regulation may function as a bioactive coating [54]. This implies that in the presence of body fluids, a layer of calcium phosphate may grow on the surface of the TiO<sub>2</sub> film, allowing the implant to bond with the surrounding bone tissues [54]. Zhao et al. [56] plasma sprayed TiO<sub>2</sub> coatings on Ti alloy substrate using nano TiO<sub>2</sub> powders as feedstocks to explore their bioactivity and cytocompatibility. They reported that the acid treatment of plasma sprayed TiO<sub>2</sub> coating using a high concentration of sulfuric acid promoted the formation of apatite on the surface. The bioactivity of TiO<sub>2</sub> could not be enhanced at a low concentration (0.01 M) of sulfuric acid (H<sub>2</sub>SO<sub>4</sub>), indicating that the concentration of H<sub>2</sub>SO<sub>4</sub> influenced the bioactivity of TiO<sub>2</sub> coatings. The in vitro cell culture test showed that the acid treatment of TiO<sub>2</sub> coatings enhanced cell adhesion. This could be attributed to the formation of many hydroxyl groups (Ti-OH bonds) on the surface of TiO<sub>2</sub> by acid treatment. The OH groups enhanced the attachment and adhesion of cells [56]. Several reports are available which revealed the formation of apatite on TiO<sub>2</sub> powders and sol-gel TiO<sub>2</sub> film [57] in SBF. Incorporating other metallic elements such as copper (Cu) into Ti-based material can accelerate cellular activity and stimulate osteogenesis (bone tissue formation). Antibacterial capabilities of Cu are extremely impressive [58]. He et al. [59] prepared Copper oxide (CuO) doped TiO<sub>2</sub> coatings on Ti-based implant material by using a combination of magnetron sputtering and annealing process. The in vitro cytocompatibility tests revealed that the TiO<sub>2</sub>/CuO coating displayed no apparent toxicity and supported osteoblast spreading and proliferation. The composite coating outperformed pure-Ti and TiO<sub>2</sub> coating in terms of corrosion resistance and antibacterial potential against *Staphylococcus aureus* bacterial species.

The possible applications of titanium dioxide nanotubes on Ti metal as bone implants was summarized in a review article by Awad et al. [51]. TiO<sub>2</sub> nanotubes of diameters ranging from 30 to 100 nm were reported to increase cell attachment and osseointegration (bonding of implant with bone tissue) [60]. TiO<sub>2</sub> nanotubes can

also be filled with drugs or modified with proteins or hydroxyapatite, making them highly essential for bone implants.

TiO<sub>2</sub> nanotubes offer greater specific surface area, that allows biomolecules to be immobilized and employed in biosensor development [61]. Biosensors are analytical devices that combine a bioreceptor (for example, a catalyst) with a transducer to transform a biological response into electrical signals [62]. Owing to the semiconducting attributes of TiO<sub>2</sub> nanotubes, the rapid transport of electrons takes place from the surface reaction to the Ti substrate. This improves the performance of the biosensor and aids in the diagnosis of diseases [63]. For instance, the immobilization of enzyme fructosyl-amino acid oxidase in TiO<sub>2</sub> nanotubes can detect glycated hemoglobin (HbA1c) in a diabetic patient [64].

The biological performance of TiO<sub>2</sub> is influenced by the surface topography and porosities [57]. Garcia-Lobato et al. [55] deposited TiO<sub>2</sub> coatings on 316 L stainless steel plates using the spraying method. The deposition rate, which is a spraying parameter, was varied. A rough and porous TiO<sub>2</sub> layer was obtained at a high deposition rate. Such a TiO<sub>2</sub> layer assisted the nucleation and growth of hydroxyapatite. According to Zhang et al. [65], a micro/nano-structured TiO<sub>2</sub> coating deposited via induction suspension plasma spraying showed better adsorption of protein than the traditional TiO<sub>2</sub> coating deposited by atmospheric plasma spraying or pure Ti with a smooth surface. The cell culture experiment showed that the micro/nano structured TiO<sub>2</sub> coating also facilitated cell attachment, proliferation, and alkaline phosphatase activity.

Metallic implants such as 316 L stainless steel are susceptible to bacterial infection and corrosion [66]. To shield the stainless steel implants from such infection and corrosion, Zhang et al. [66] developed a titanium oxide-polytetrafluoroethylene (TiO<sub>2</sub>-PTFE) nanocomposite coating on a polydopamine coated stainless steel using a sol-gel dip coating process. Under UV radiation, TiO<sub>2</sub> nanoparticles inhibited the growth of bacteria. The TiO<sub>2</sub>-PTFE coating exhibited excellent antibacterial and anti-adhesion characteristics against both *Escherichia coli* and *Staphylococcus aureus* bacterial strains. The coating also displayed remarkable corrosion resistance in SBF.

## 2.4 Pigments

TiO<sub>2</sub> exhibits a high refractive index, whiteness, brightness, high opacity, and non-toxicity which make it suitable to be used as white pigments [67]. The high brightness and opacity of TiO<sub>2</sub> can be ascribed to its tendency to scatter light [68]. TiO<sub>2</sub> pigments are often used in paints, coatings, inks, paper, plastics, cosmetics, etc. [1]. According to Fresnel, the larger the refractive index difference between the pigment and the medium, the more light is reflected from the surface and the opacity is enhanced [69]. The refractive indices of rutile and anatase TiO<sub>2</sub> pigments are 2.73 and 2.55, respectively. The particle size of TiO<sub>2</sub> and its dispersion (interparticle separation) have a significant impact on the degree of scattering of light. It has been shown that efficient light scattering of a particular wavelength occurs when the particle size is approximately half that wavelength. As a result, the optimum pigment size for the maximum scattering of visible light is 0.2–0.3 μm. The agglomeration of TiO<sub>2</sub> particles weakens the hiding power of TiO<sub>2</sub> [1]. The degree of the pigment dispersion affects the opacity, tinting strength, brightness, gloss development, and durability of the TiO<sub>2</sub> film. Therefore, the maximum opacity and other essential optical and physical properties in a coating can be achieved by completely dispersing TiO<sub>2</sub> pigments down to their ultimate particle size [69]. The increase in the particle size of TiO<sub>2</sub> above 1 μm harms the film gloss and the degree of dispersion [1]. In addition to TiO<sub>2</sub>, some fine particle minerals, also known as pigment

extenders, are used as fillers in paints to enhance the optical properties of TiO<sub>2</sub>. These pigment extenders avoid the agglomeration of TiO<sub>2</sub> particles and separate the individual particles of TiO<sub>2</sub> to obtain the optimum inter-particle spacing required for maximum opacity. Some of the examples of minerals include calcium carbonate (CaCO<sub>3</sub>), silica, kaolin, talc, wollastonite, mica, and so on [1]. Some of the ways of fabricating mineral-TiO<sub>2</sub> composites include the mechano-chemical method, chemical precipitation method, etc. Currently, the mineral-TiO<sub>2</sub> composite pigment is used in coatings, plastics, and papermaking [70].

Zhou et al. [71] synthesized barite/TiO<sub>2</sub> composite particles using the chemical precipitation method. Barite and TiO<sub>2</sub> were joined together with the Ti-O-Ba bond. The pigment properties of the composite, such as hiding power and oil adsorption value were 18.5 g/m<sup>2</sup> and 15.5 g/100 g, respectively which were comparable to the pigment properties of TiO<sub>2</sub>. Using the same approach, Chen et al. [72] fabricated CaCO<sub>3</sub> based-TiO<sub>2</sub> pigment and observed that the hiding power of the end product (23.82 g/m<sup>2</sup>) was similar to that of anatase TiO<sub>2</sub> (22.56 g/m<sup>2</sup>). Similarly, the illite/TiO<sub>2</sub> composite pigment offered higher whiteness of 95.73% and hiding power of 97.55% than illite [73]. These results indicated that composite pigments could be used in applications, including architectural paints, whitening additives in paper manufacturing, etc.

Wang et al. [67] studied the pigment properties of a mechano-chemically formulated calcined kaolin/TiO<sub>2</sub> composite. The composite showed the whiteness and hiding power of 95.7%, and 17.12 g/m<sup>2</sup>, respectively which was close to the pigment properties of pure anatase TiO<sub>2</sub> which offered a whiteness of 95.8%, and hiding power of 15.14 g/m<sup>2</sup>. Similar pigment properties were also observed for brucite/TiO<sub>2</sub> composite, wollastonite/anatase TiO<sub>2</sub> composite, and sericite/anatase TiO<sub>2</sub> composite [70]. However, amorphous silica/anatase TiO<sub>2</sub> composite displayed an even better hiding power of 13.07 g/m<sup>2</sup> as compared to pure anatase TiO<sub>2</sub> [74].

Sun et al. [75] adopted another technique called the self-assembly method to fabricate barite/rutile TiO<sub>2</sub> composite. As compared to pure rutile TiO<sub>2</sub>, the composite product possessed identical pigment attributes (hiding strength of 12.08 g/m<sup>2</sup> and oil adsorption value of 14.48 g/100 g). Consequently, these composites could easily substitute pure TiO<sub>2</sub> as additives in paper manufacturing industries.

According to Hou et al. [76], the whiteness of TiO<sub>2</sub>/wollastonite composite (96.6%) was somewhat higher than that of anatase TiO<sub>2</sub> (96.2%). Therefore, the TiO<sub>2</sub>/wollastonite composites could also be used as pigments in coatings.

The dispersion of TiO<sub>2</sub> particles (5–10 vol. %) in a molten glass phase provides whiteness and opacity. These enamels (or glass phases) are coated on metals or ceramics. A desirable whiteness and appearance in enamels can be achieved by controlling the anatase-to-rutile phase ratio. In paper manufacturing industries, pigment coatings are added to improve the printability, smoothness, brightness, and opacity of the paper. A smooth paper surface is obtained by adding TiO<sub>2</sub> pigments. TiO<sub>2</sub> pigments are also added to the textiles fibers to impart opacity and provide protection against visible and UV light. The content of the pigments in the textile fibers ranges from 0.3 to 1 wt. % [1]. TiO<sub>2</sub> pigments are also utilized in artificial leather, cement products, ceramics, glass, cosmetics, laminating papers, pharmaceuticals, moldings, bitumen floorings, printing inks, rubber, putty, shoe creams, etc. [69].

## **2.5 Wear resistant**

When two solid bodies in contact have relative motion, some material is removed from their surfaces [77]. This phenomenon of material removal from the

surface owing to rubbing is known as wear. Many engineering components made of metals or alloys fail or their service life is reduced due to wear [78]. So, efforts should be undertaken to minimize this undesirable phenomenon [79]. One method to combat wear is by modifying the surface properties of the material to impart anti-wear characteristics [80]. For instance, depositing a new hard and wear-resistant material onto the substrate can significantly reduce the wear of the substrate material. TiO<sub>2</sub> possesses high hardness and is known to resist wear [81]. Thermally sprayed TiO<sub>2</sub> coatings are often used as wear-resistant coatings in pump seal, propeller shaft-bearing sleeve, etc. [82]. To reduce wear, researchers have employed different methods to produce TiO<sub>2</sub> coatings.

The rutile TiO<sub>2</sub> phase offers low friction and high wear-reducing abilities [83]. It can be produced by the thermal oxidation of Ti-alloys. Krishna et al. [81] deposited Ti coatings on stainless steel by magnetron sputtering. The Ti coating was later converted to TiO<sub>2</sub> by thermal oxidation at 550°C. As-deposited TiO<sub>2</sub> layer exhibited a much higher hardness of 11 GPa (4 times that of the as-deposited Ti), which was close to the hardness of the bulk rutile TiO<sub>2</sub> phase. This enhanced the load-carrying capacity of the oxidized specimen. Sun et al. [84] also fabricated rutile TiO<sub>2</sub> by thermally oxidizing pre-coated titanium on an aluminum alloy (Al-alloy) substrate. For tribological testing, an alumina counterball was used. Severe adhesive wear with stick-slip propensity and high friction (friction coefficient of 0.5–0.8) were reported for the uncoated Al-alloy. Thermally oxidized coatings showed three orders of magnitude reduction in wear rate with no signs of adhesive wear. The oxidized coating offered less friction (friction coefficient  $\mu < 0.25$ ), and it did not fail throughout the test. High hardness was responsible for the excellent wear-resistant of the oxidized coatings. Other researchers have also documented the role of thermally oxidized Ti in combating wear [85].

Dejang et al. [86] fabricated Al<sub>2</sub>O<sub>3</sub>/TiO<sub>2</sub> composite coating with varying contents of TiO<sub>2</sub> (0–20 wt. %) using plasma spraying process and compared its wear performance with monolithic Al<sub>2</sub>O<sub>3</sub> coatings. The hardness of the composite coating was found to be lower than that of Al<sub>2</sub>O<sub>3</sub> coating owing to the comparatively lower hardness of TiO<sub>2</sub> compared to Al<sub>2</sub>O<sub>3</sub>. On the other hand, the fracture toughness was improved by increasing the weight fraction of TiO<sub>2</sub>. However, the sliding wear test revealed that the wear rate of Al<sub>2</sub>O<sub>3</sub> coating was 1.5 times higher than that of 3 wt. % TiO<sub>2</sub> doped Al<sub>2</sub>O<sub>3</sub> composite coatings owing to the presence of TiO<sub>2</sub> splats that increased the fracture toughness and decreased the friction coefficient. Owing to the hydrophilic nature, TiO<sub>2</sub> layer can absorb moisture from the air and potentially lowers the friction coefficient.

Baghery et al. [87] used the electrodeposition method to deposit nickel-titania (Ni-TiO<sub>2</sub>) nano composite coating. They discovered that increasing the quantity of TiO<sub>2</sub> nanoparticles increased microhardness and wear resistance. The grain refinement and dispersion strengthening mechanisms were responsible for the increase in hardness. Similar strengthening mechanisms were also reported for TiO<sub>2</sub> sol-strengthened copper-tin-polytetrafluoroethylene (Cu-Sn-PTFE) composite coating by Ying et al. [88]. Baghery et al. [87] further observed that the stable friction coefficient for Ni coating was 1 that was reduced to 0.3 for Ni-8.3 wt. % TiO<sub>2</sub> coating. The TiO<sub>2</sub> nanoparticle reinforcement in the coating minimized the direct interaction between the Ni matrix and the abrasive counterbody. Furthermore, TiO<sub>2</sub> nanoparticles detached from the coating due to abrasive action served as a solid lubricant between the two mating surfaces. These mechanisms reduced the friction coefficient and wear rate for TiO<sub>2</sub> doped coatings. Similarly, Li et al. [89] plasma-sprayed chromium oxide (Cr<sub>2</sub>O<sub>3</sub>) - TiO<sub>2</sub> composite coatings and found that Cr<sub>2</sub>O<sub>3</sub> doped with 16 wt. % TiO<sub>2</sub> coatings exhibited the lowest friction coefficient owing to its minimum surface free energy. The presence of (Cr<sub>0.88</sub>Ti<sub>0.12</sub>)<sub>2</sub>O<sub>3</sub> phase

raised the microhardness of the composite coatings while lowered their friction coefficient. Babu et al. [90] examined the tribological performance of TiO<sub>2</sub> coated aluminum-silicon carbide (Al-SiC) substrate and uncoated Al-SiC. They reported that the plasma sprayed TiO<sub>2</sub> coating (570 HV<sub>0.5</sub>) had an 8-fold higher hardness than the Al-SiC substrate (70 HV<sub>0.5</sub>). This resulted in the reduction in wear rate from 11 mm<sup>3</sup>/m for the uncoated specimen to 6 mm<sup>3</sup>/m for the coated specimens. The uncoated sample experienced severe abrasive wear with delamination. The plasma-sprayed sample, on the other hand, showed only minor abrasive wear. Ying et al. [88] investigated the wear performance of electrodeposited Cu-Sn-PTFE coating with TiO<sub>2</sub> sol as a reinforcing agent. At 40 ml/L concentration of TiO<sub>2</sub> sol, TiO<sub>2</sub> nanoparticles were found to be well dispersed which strengthened the Cu-Sn-PTFE matrix. This led to an increment in hardness and wear resistance of the TiO<sub>2</sub> doped composite coating. The wear performance of TiO<sub>2</sub> film deposited on commercially pure Ti using the sol-gel method was evaluated by Comakli et al. [91]. The TiO<sub>2</sub> coated specimen showed a low value of friction coefficient because of the self-lubricating property of TiO<sub>2</sub> films, and higher surface hardness than the uncoated specimen. In another investigation, similar results of TiO<sub>2</sub> films improving tribological performance have been published [92]. Barkallah et al. [93] fabricated aluminum oxide/tricalcium phosphate (Al<sub>2</sub>O<sub>3</sub>/10 wt.% TCP) bioceramic for an orthopedic implant and found that the wear behavior of the biocoating could be improved by incorporating 5 wt.% TiO<sub>2</sub>. The hardness and the fracture toughness of the bioceramic without TiO<sub>2</sub> were 3.56 GPa and 8.734 MPa m<sup>1/2</sup>, respectively. Both hardness and fracture toughness were increased to 8.55 GPa (140% increment) and 13 MPa m<sup>1/2</sup> (48.8% increment) when 5 wt. % TiO<sub>2</sub> was added. This increment in hardness and fracture toughness could be responsible for the improved wear performance. As a result, by adding TiO<sub>2</sub>, the tribological performance of composite can be significantly improved.

## 2.6 Gas sensing

TiO<sub>2</sub> was widely studied by numerous researchers for gas sensing performance as well [94]. The working principle of the TiO<sub>2</sub> metal oxide gas sensor involves adsorption, desorption reactions relevant to air and test gas of interest [94]. TiO<sub>2</sub> surface at ambient temperature consists of adsorption of ambient oxygen in the form of O<sub>2</sub> [94]. This is termed as physically adsorbed oxygen [94]. TiO<sub>2</sub> surface, at elevated temperatures (150–450°C), consists of electron transfer as a result of chemical interaction of ambient oxygen that ultimately leads to the formation of chemical adsorbed oxygen in different forms namely, O<sub>2</sub><sup>-</sup>, O<sup>-</sup> [94]. This leads to an increase in the sensor resistance under the influence of air (R<sub>a</sub>). During gas sensing, test gas such as hydrogen (H<sub>2</sub>) reacts with chemically adsorbed oxygen ions to form an oxidized reaction product and this reaction transports electrons back to the conduction band of the TiO<sub>2</sub> layer [94]. Herein, sensor resistance of TiO<sub>2</sub> under the influence of test gas (denoted as R<sub>g</sub>) drops to a certain value depending upon the test gas concentration and the change in the electrical signal from R<sub>a</sub> to R<sub>g</sub> ultimately determines gas response (R<sub>a</sub>/R<sub>g</sub>) or (R<sub>a</sub>-R<sub>g</sub>)/R<sub>a</sub> [94].

In line with this principle, TiO<sub>2</sub> has been studied by numerous researchers for H<sub>2</sub> [94], carbon monoxide (CO) [95], ammonia (NH<sub>3</sub>) [96], etc. In addition, TiO<sub>2</sub> is one of the popular materials for developing air-fuel ratio sensors [97]. A brief review of TiO<sub>2</sub> sensors in the recent literature is detailed in the following paragraphs:

Hydrogen (H<sub>2</sub>): H<sub>2</sub> being colorless, odorless, highly combustible gas needs careful attention during its generation, storage, transportation as well [98]. Therefore,

considerable efforts have been made by researchers to develop H<sub>2</sub> sensors using TiO<sub>2</sub> in different forms [94]. Tang et al. deposited TiO<sub>2</sub> anatase film using reactive triode sputtering and reported H<sub>2</sub> sensing response at 370°C. Though this paper reported the possibility of TiO<sub>2</sub> films towards H<sub>2</sub> sensing, gas sensing performance was not investigated in detail [99]. Devi et al. reported the synthesis of mesoporous TiO<sub>2</sub> powders and obtained gas response ( $R_a/R_g \sim 4.8$ ) was found superior to that of commercial TiO<sub>2</sub> powder ( $R_a/R_g \sim 2.5$ ) [100]. This was attributed to the larger surface area for efficient gas sensing reactions [100]. Yoo et al. synthesized a nano-fibrillar TiO<sub>2</sub> sensor for H<sub>2</sub> sensing applications at 400°C [101]. Jun et al. reported the H<sub>2</sub> sensing behavior of TiO<sub>2</sub> films grown using the thermal oxidation route and studied the analogy between gas sensor response and film microstructure. Superior H<sub>2</sub> sensor response ( $R_a/R_g$  of  $1.2 \times 10^6$ ) at 300°C with a response time of 10 s was attributed to the ease of H<sub>2</sub> penetration into the sensing layer owing to its porous morphology [102]. Moon et al. reported a gas sensor response of 250% for TiO<sub>2</sub> film exposed to 100 ppm H<sub>2</sub> gas at 200°C [103]. Moon et al. synthesized meso-porous TiO<sub>2</sub> film by anodization over Ti substrate and reported gas response ( $R_a/R_g \sim 2.5$ ) at 140°C towards 1000 ppm H<sub>2</sub> [104]. In this report, the enhanced H<sub>2</sub> response could be attributed to the mesoporous microstructure of TiO<sub>2</sub> film. The effect of niobium (Nb) doping with TiO<sub>2</sub> film was reported to yield a useful gas response at room temperature [105]. The plausible reason behind room temperature sensing can be attributed to enhanced oxygen adsorption over TiO<sub>2</sub> nanotubes.

Carbon monoxide (CO) is also a colorless, odorless, toxic gas that needs early detection [106]. Harmful levels of CO could be found owing to gasoline engine exhaust, burning of coal in a boiler room, wooden stove exhaust, cigarette smoke, etc. [107]. Quite a few researchers have studied TiO<sub>2</sub> for CO sensing applications. Devi et al. developed a mesoporous TiO<sub>2</sub> particulate sensor and obtained gas response in the presence of 500 ppm CO was ( $R_a/R_g \sim 2.4$ ) at 450°C [100]. Jun et al. prepared TiO<sub>2</sub> film using the micro-arc oxidation method and reported gas response of ( $R_a/R_g \sim 3.10$ ) towards 30 ppm CO at 350°C [95]. Choi et al. observed gas response of ( $R_a/R_g \sim 1.4$ ) at 600°C towards 500 ppm CO using 7.5 wt. % Al-doped TiO<sub>2</sub> sensor using an auto combustion route [108].

Ammonia (NH<sub>3</sub>) is a volatile organic compound and being highly flammable and harmful to the respiratory system needs careful monitoring during its handling [109]. TiO<sub>2</sub> has been explored by different researchers for NH<sub>3</sub> sensing applications. Karunagaran et al. deposited TiO<sub>2</sub> thin film using DC magnetron sputtering [96]. A sensitivity factor of 7000 was noted at a temperature of 300°C towards 500 ppm NH<sub>3</sub> [96]. Gardon et al. deposited TiO<sub>2</sub> layer using atmospheric plasma spraying method in which maximum gas response ( $(R_a - R_g)/R_a$ ) of 7% was attained at 210°C [110]. Dhivya et al. tested NH<sub>3</sub> sensing performance of DC magnetron sputtered TiO<sub>2</sub> film with a gas response ( $R_a/R_g \sim 8000$ ) measured at room temperature [111].

In practice, the TiO<sub>2</sub> functional layer finds application as a lambda sensor in the automotive exhaust system between the exhaust manifold and catalytic converter [112]. Herein, the term lambda (designated as 'λ') refers to the air-fuel equivalence ratio that measures the oxygen content in the exhaust gas being analyzed [113]. The lambda sensor is used to properly adjust the fuel amount that is being supplied to the cylinder of the internal combustion engine [114]. This controls the air-fuel mixture thereby ensuring the proper running of the engine [115]. Also, the lambda sensor is used to ensure that the catalytic converter is functioning in an intended manner [116]. The following paragraph presents a review of successful attempts to make TiO<sub>2</sub> based lambda sensors.

In the year 1987, a group of inventors in Japan developed porous TiO<sub>2</sub> coating as lambda sensor to measure air-fuel equivalence ratio at around 1000°C. TiO<sub>2</sub>

(50  $\mu\text{m}$ ) film was coated over commercially available  $\text{Al}_2\text{O}_3$  substrate having a pair of platinum (Pt) electrodes. As a result of the change in  $\lambda$  from 1.2 to 0.7, sensor resistance first increased from 10 to  $10^4 \Omega$ , reached a saturation value. Upon the change in  $\lambda$  from 0.7 to 1.2, sensor resistance again decreased from  $10^4 \Omega$  to the original value, i.e. 10  $\Omega$ . Thus, the proposed sensor was a potential candidate to function as a lambda sensor in real-time applications [117].

Francioso et al. developed  $\text{TiO}_2$  thin film through the sol-gel route and tested its potential for lambda measurements in real-time applications [113]. Initially, the variation of sensor resistance at 650°C to different nitrogen/oxygen concentrations corresponding to different  $\lambda$  values was measured. In the next step, the dynamic response of the lambda sensor was also measured for the mixture of nitrogen ( $\text{N}_2$ ), oxygen ( $\text{O}_2$ ), carbon dioxide ( $\text{CO}_2$ ), nitrogen oxide (NO), and methane ( $\text{CH}_4$ ) for different  $\lambda$  values. In both cases, namely, under exposure to nitrogen/oxygen mixture and mixture of said gases, the change in sensor resistance was almost similar. Therefore, this work proved the potential of  $\text{TiO}_2$  thin film as a lambda sensor [113]. However, the repeatability and stability of the sensor needed improvement owing to the instability of gold electrodes.

In successive attempts, Francioso et al. deposited sol-gel  $\text{TiO}_2$  thin film with Pt electrodes [115]. Experiments were performed at varying temperatures (400–700°C) in the presence of 0.1% of  $\text{O}_2$ . Since maximum gas response determined by the ratio of electric current in the presence of  $\text{O}_2$  to that of  $\text{N}_2$  ( $I_{\text{O}_2}/I_{\text{N}_2}$ ) was realized at 650°C, the sensor was tested at different  $\text{O}_2$  concentrations in the range of 0.2–0.5%. Sensing tests were carried out for other gases, namely,  $\text{CH}_4$ ,  $\text{CO}_2$ , oxides of nitrogen ( $\text{NO}_x$ ) to ascertain the suitability of the sensor. Sensor performance was finally compared to commercial lambda sensors that showed close agreement between sensing signals [115].

### 3. Conclusions

This chapter demonstrated the potential of titanium dioxide ( $\text{TiO}_2$ ) in imparting UV protection, anti-wear, corrosion inhibitor, gas detection properties. In the mechanical sector,  $\text{TiO}_2$  can be used as a corrosion and wear-resistant material.  $\text{TiO}_2$  coatings protect the substrate from the corrosive medium by serving as a ceramic barrier and also provide cathodic protection to the metals under UV illumination because of the photo-electrochemical property of  $\text{TiO}_2$ . A tremendous increment in the corrosion resistance of the sample with the application of  $\text{TiO}_2$  coatings proved the potential of  $\text{TiO}_2$  as a corrosion inhibitor.  $\text{TiO}_2$ , owing to its high hardness, fracture toughness can be embedded in a composite to improve the tribological performance of functional layers in numerous applications.  $\text{TiO}_2$  is also found to be a suitable candidate for bone implants. The bioactivity tests revealed that the acid treatment of  $\text{TiO}_2$  enhances the cell attachment and the bonding of the implant with the bone tissues. Owing to the high refractive index,  $\text{TiO}_2$  layers are applied in sunscreens to protect the human skin from harmful UV rays.  $\text{TiO}_2$  is also incorporated in textiles to reduce its photochemical degradation and therefore its mechanical properties are retained even after exposure to UV light. The whiteness, brightness, and hiding power of  $\text{TiO}_2$  pigments are utilized in paints, coatings, papers, textile industries, etc. By adding certain minerals the degree of dispersion of  $\text{TiO}_2$  pigments can be improved that further enhances the pigment properties of  $\text{TiO}_2$ . The change in the electrical resistance of  $\text{TiO}_2$  layers was exploited to develop a gas sensor for air quality monitoring and a lambda sensor for monitoring of air-fuel ratio of internal combustion engines.  $\text{TiO}_2$  nanoparticles have been found to outperform their bulk counterparts in such applications, which can be attributed to their large surface area to volume ratio.

## List of nomenclatures

TiO <sub>2</sub>	Titanium oxide
NaCl	Sodium Chloride
Mg	Magnesium
MgTiO <sub>3</sub>	Magnesium titanate
Ni-W	Nickel-Tungsten
ZrO <sub>2</sub>	Zirconium oxide
Al <sub>2</sub> O <sub>3</sub>	Aluminum oxide/Alumina
Zn	Zinc
ZnO	Zinc Oxide
n-TiO <sub>2</sub>	Nano titania
micro-TiO <sub>2</sub>	Micron-sized titania
TiNi	Nitinol
HCl	Hydrochloric acid
H <sub>2</sub> SO <sub>4</sub>	Sulfuric acid
OH	Hydroxyl
Cu	Copper
Ti	Titanium
CuO	Copper oxide
TiO <sub>2</sub> -PTFE	Titanium oxide-polytetrafluoroethylene
CaCO <sub>3</sub>	Calcium carbonate
Cu-Sn-PTFE	Copper-tin-polytetrafluoroethylene
Cr <sub>2</sub> O <sub>3</sub>	Chromium oxide
Al-SiC	Aluminum-Silicon carbide
H <sub>2</sub>	Hydrogen
CO	Carbon monoxide
NH <sub>3</sub>	Ammonia
Nb	Niobium
N <sub>2</sub>	Nitrogen
O <sub>2</sub>	Oxygen
CO <sub>2</sub>	Carbon dioxide
NO	Nitrogen oxide
CH <sub>4</sub>	Methane
Pt	Platinum
NO <sub>x</sub>	Oxides of Nitrogen
R <sub>a</sub>	Electrical resistance of TiO <sub>2</sub> under the influence of air
R <sub>g</sub>	Electrical resistance of TiO <sub>2</sub> under the influence of test gas
λ	Air-fuel equivalence ratio
I <sub>O2</sub>	Electrical current of TiO <sub>2</sub> under the influence of oxygen
I <sub>N2</sub>	Electrical current of TiO <sub>2</sub> under the influence of nitrogen
UV	Ultraviolet
UVA	Ultraviolet A
UVB	Ultraviolet B
UVC	Ultraviolet C
UPF	Ultraviolet Protection Factor
PACVD	Plasma Assisted Chemical Vapor Deposition
ALD	Atomic Layer Deposition
XRD	X-Ray Diffraction
GO	Graphene Oxide
EIS	Electrochemical Impedance Spectroscopy
HA	Hydroxyapatite
PDMAS	Poly-dimethylaminosiloxane

SEM	Scanning Electron Microscope
EDS	Energy-Dispersive X-Ray Spectroscopy
PEEK	Polyetheretherketone
PET	Polyester
SPF	Sun Protection Factor
NR	Natural Rubber
SBF	Simulated Body Fluid
PTFE	Polytetrafluoroethylene
TCP	Tricalcium Phosphate

IntechOpen

IntechOpen

### **Author details**

Rajib Das, Vibhav Ambardekar\* and Partha Pratim Bandyopadhyay  
Department of Mechanical Engineering, Indian Institute of Technology,  
Kharagpur, India

\*Address all correspondence to: vibhav6305@gmail.com

### **IntechOpen**

© 2021 The Author(s). Licensee IntechOpen. This chapter is distributed under the terms of the Creative Commons Attribution License (<http://creativecommons.org/licenses/by/3.0>), which permits unrestricted use, distribution, and reproduction in any medium, provided the original work is properly cited. 

## References

- [1] P. Blanchart, Extraction, Properties and Applications of TiO<sub>2</sub>, in: *Ind. Chem. Oxides Emerg. Appl.*, John Wiley & Sons Ltd, Chichester, UK, 2018: pp. 255-309. <https://doi.org/10.1002/9781119424079.ch6>.
- [2] M. Gardon, J.M. Guilemany, Milestones in functional titanium dioxide thermal spray coatings: A review, *J. Therm. Spray Technol.* 23 (2014) 577-595. <https://doi.org/10.1007/s11666-014-0066-5>.
- [3] M. Robotti, *Functional surfaces obtained by thermal spray techniques*, University of Barcelona, 2016.
- [4] A.J. Haider, Z.N. Jameel, I.H.M. Al-Hussaini, Review on: Titanium Dioxide Applications, *Energy Procedia.* 157 (2019) 17-29. <https://doi.org/10.1016/j.egypro.2018.11.159>.
- [5] U.R. Evans, Electrochemical Mechanism of Atmospheric Rusting, *Nature.* 206 (1965) 980-982.
- [6] S. Kar, S. Paul, P.P. Bandyopadhyay, Processing and characterisation of plasma sprayed oxides: Microstructure, phases and residual stress, *Surf. Coatings Technol.* 304 (2016) 364-374. <https://doi.org/10.1016/j.surfcoat.2016.07.043>.
- [7] P. Das, S. Paul, P.P. Bandyopadhyay, Preparation of diamond reinforced metal powders as thermal spray feedstock using ball milling, *Surf. Coatings Technol.* 289 (2016) 165-171. <https://doi.org/10.1016/j.surfcoat.2015.12.022>.
- [8] A. Pilbáth, L. Nyikos, I. Bertóti, E. Kálmán, Zinc corrosion protection with 1,5-diphosphono-pentane, *Corros. Sci.* 50 (2008) 3314-3321. <https://doi.org/10.1016/j.corsci.2008.09.021>.
- [9] T.-K. Yeh, Y.-C. Chien, B.-Y. Wang, C.-H. Tsai, Electrochemical characteristics of zirconium oxide treated Type 304 stainless steels of different surface oxide structures in high temperature water, *Corros. Sci.* 50 (2008) 2327-2337. <https://doi.org/10.1016/j.corsci.2008.05.012>.
- [10] S. Datta, D.K. Pratihari, P.P. Bandyopadhyay, Modeling of input-output relationships for a plasma spray coating process using soft computing tools, *Appl. Soft Comput. J.* 12 (2012) 3356-3368. <https://doi.org/10.1016/j.asoc.2012.07.015>.
- [11] P.P. Bandyopadhyay, S. Siegmann, Friction and wear behavior of vacuum plasma-sprayed Ti-Zr-Ni quasicrystal coatings, *Surf. Coatings Technol.* 197 (2005) 1-9. <https://doi.org/10.1016/j.surfcoat.2004.11.009>.
- [12] M. Hadad, P.P. Bandyopadhyay, J. Michler, J. Lesage, Tribological behaviour of thermally sprayed Ti-Cr-Si coatings, *Wear.* 267 (2009) 1002-1008. <https://doi.org/10.1016/j.wear.2009.01.013>.
- [13] H. Yun, J. Li, H.-B. Chen, C.-J. Lin, A study on the N-, S- and Cl-modified nano-TiO<sub>2</sub> coatings for corrosion protection of stainless steel, *Electrochim. Acta.* 52 (2007) 6679-6685. <https://doi.org/10.1016/j.electacta.2007.04.078>.
- [14] P. Furman, J. Gluszek, J. Masalski, Titanium dioxide film obtained using the MOCVD method on 316L steel, *J. Mater. Sci. Lett.* 16 (1997) 471-472. <https://doi.org/10.1023/A:1018564326769>.
- [15] S. Ghosh, S. Das, T.K. Bandyopadhyay, P.P. Bandyopadhyay, A.B. Chattopadhyay, Indentation responses of plasma sprayed ceramic coatings, *J. Mater. Sci.* 38 (2003) 1565-1572. <https://doi.org/10.1023/A:1022997203996>.

- [16] P.P. Bandyopadhyay, Processing and Characterisation of Plasma Sprayed Ceramic Coatings on Steel Substrate, Dr. Diss. (2000).
- [17] D. Yan, J. He, X. Li, Y. Liu, J. Zhang, H. Ding, An investigation of the corrosion behavior of Al<sub>2</sub>O<sub>3</sub>-based ceramic composite coatings in dilute HCl solution, *Surf. Coatings Technol.* 141 (2001) 1-6. [https://doi.org/10.1016/S0257-8972\(01\)01170-7](https://doi.org/10.1016/S0257-8972(01)01170-7).
- [18] Y. Ohko, S. Saitoh, T. Tatsuma, A. Fujishima, Photoelectrochemical Anticorrosion and Self-Cleaning Effects of a TiO<sub>2</sub> Coating for Type 304 Stainless Steel, *J. Electrochem. Soc.* 148 (2001) B24. <https://doi.org/10.1149/1.1339030>.
- [19] G.X. Shen, Y.C. Chen, C.J. Lin, Corrosion protection of 316 L stainless steel by a TiO<sub>2</sub> nanoparticle coating prepared by sol-gel method, *Thin Solid Films.* 489 (2005) 130-136. <https://doi.org/10.1016/j.tsf.2005.05.016>.
- [20] Y. Sun, Thermally oxidised titanium coating on aluminium alloy for enhanced corrosion resistance, *Mater. Lett.* 58 (2004) 2635-2639. <https://doi.org/10.1016/j.matlet.2004.04.001>.
- [21] M.G. Mahmoud, R. Wang, M. Kato, K. Nakasa, Influence of ultraviolet light irradiation on corrosion behavior of weathering steel with and without TiO<sub>2</sub>-coating in 3mass% NaCl solution, *Scr. Mater.* 53 (2005) 1303-1308. <https://doi.org/10.1016/j.scriptamat.2005.07.039>.
- [22] C.X. Shan, X. Hou, K.L. Choy, Corrosion resistance of TiO<sub>2</sub> films grown on stainless steel by atomic layer deposition, *Surf. Coatings Technol.* 202 (2008) 2399-2402. <https://doi.org/10.1016/j.surfcoat.2007.08.066>.
- [23] Z. Yu, H. Di, Y. Ma, Y. He, L. Liang, L. Lv, X. Ran, Y. Pan, Z. Luo, Preparation of graphene oxide modified by titanium dioxide to enhance the anti-corrosion performance of epoxy coatings, *Surf. Coatings Technol.* 276 (2015) 471-478. <https://doi.org/10.1016/j.surfcoat.2015.06.027>.
- [24] S.Z. Khalajabadi, N. Ahmad, A. Yahya, M.A.M. Yajid, A. Samavati, S. Asadi, A. Arafat, M.R. Abdul Kadir, The role of TiO<sub>2</sub> on the microstructure, biocorrosion and mechanical properties of Mg/HA-based nanocomposites for potential application in bone repair, *Ceram. Int.* 42 (2016) 18223-18237. <https://doi.org/10.1016/j.ceramint.2016.08.146>.
- [25] S. Shajahan, A. Basu, Corrosion, oxidation and wear study of electro-co-deposited ZrO<sub>2</sub>-TiO<sub>2</sub> reinforced Ni-W coatings, *Surf. Coatings Technol.* 393 (2020). <https://doi.org/10.1016/j.surfcoat.2020.125729>.
- [26] M. Poorraeisi, A. Afshar, The study of electrodeposition of hydroxyapatite-ZrO<sub>2</sub>-TiO<sub>2</sub> nanocomposite coatings on 316 stainless steel, *Surf. Coatings Technol.* 339 (2018) 199-207. <https://doi.org/10.1016/j.surfcoat.2018.02.030>.
- [27] A.M. Fadl, M.I. Abdou, M.A. Hamza, S.A. Sadeek, Corrosion-inhibiting, self-healing, mechanical-resistant, chemically and UV stable PDMAS/TiO<sub>2</sub> epoxy hybrid nanocomposite coating for steel petroleum tanker trucks, *Prog. Org. Coatings.* 146 (2020) 105715. <https://doi.org/10.1016/j.porgcoat.2020.105715>.
- [28] N.G. Krishna, R.P. George, J. Philip, Anomalous enhancement of corrosion resistance and antibacterial property of commercially pure Titanium (CP-Ti) with nanoscale rutile TiO<sub>2</sub> film, *Corros. Sci.* 172 (2020) 108678. <https://doi.org/10.1016/j.corsci.2020.108678>.
- [29] M. Merisalu, L. Aarik, J. Kozlova, H. Mändar, A. Tarre, V. Sammelselg, Effective corrosion protection of aluminum alloy AA2024-T3 with novel thin nanostructured oxide coating, *Surf.*

Coatings Technol. 411 (2021). <https://doi.org/10.1016/j.surfcoat.2021.126993>.

[30] L. Paussa, L. Guzman, E. Marin, N. Isomaki, L. Fedrizzi, Protection of silver surfaces against tarnishing by means of alumina/TiO<sub>2</sub>-nanolayers, Surf. Coatings Technol. 206 (2011) 976-980. <https://doi.org/10.1016/j.surfcoat.2011.03.101>.

[31] E. Marin, L. Guzman, A. Lanzutti, W. Ensinger, L. Fedrizzi, Multilayer Al<sub>2</sub>O<sub>3</sub>/TiO<sub>2</sub> Atomic Layer Deposition coatings for the corrosion protection of stainless steel, Thin Solid Films. 522 (2012) 283-288. <https://doi.org/10.1016/j.tsf.2012.08.023>.

[32] J. Li, J. Li, Q. Li, H. Zhou, G. Wang, X. Peng, W. Jin, Z. Yu, P.K. Chu, W. Li, TiO<sub>2</sub>-zinc phosphate/nanocrystalline zinc composite coatings for corrosion protection of biomedical WE43 magnesium alloy, Surf. Coatings Technol. 410 (2021). <https://doi.org/10.1016/j.surfcoat.2021.126940>.

[33] Q. Chen, G.D. McEwen, N. Zaveri, R. Karpagavalli, A. Zhou, Corrosion Resistance of Ti6Al4V with Nanostructured TiO<sub>2</sub> Coatings, First Edit, Elsevier Inc., 2012. <https://doi.org/10.1016/B978-1-4557-7862-1.00009-2>.

[34] T.V. Torbati, V. Javanbakht, Fabrication of TiO<sub>2</sub>/Zn<sub>2</sub>TiO<sub>4</sub>/Ag nanocomposite for synergic effects of UV radiation protection and antibacterial activity in sunscreen, Colloids Surfaces B Biointerfaces. 187 (2020) 110652. <https://doi.org/10.1016/j.colsurfb.2019.110652>.

[35] N. Sabzevari, S. Qiblawi, S.A. Norton, D. Fivenson, Sunscreens: UV filters to protect us: Part 1: Changing regulations and choices for optimal sun protection, Int. J. Women's Dermatology. 7 (2021) 28-44. <https://doi.org/10.1016/j.ijwd.2020.05.017>.

[36] H. Yang, S. Zhu, N. Pan, Studying the mechanisms of titanium dioxide as ultraviolet-blocking additive for films and fabrics by an improved scheme, J. Appl. Polym. Sci. 92 (2004) 3201-3210. <https://doi.org/10.1002/app.20327>.

[37] Y. Li, W. Xie, X. Hu, G. Shen, X. Zhou, Y. Xiang, X. Zhao, P. Fang, Comparison of Dye Photodegradation and its Coupling with Light-to-Electricity Conversion over TiO<sub>2</sub> and ZnO, Langmuir. 26 (2010) 591-597. <https://doi.org/10.1021/la902117c>.

[38] X. Wang, Z. Li, J. Shi, Y. Yu, One-Dimensional Titanium Dioxide Nanomaterials: Nanowires, Nanorods, and Nanobelts, Chem. Rev. 114 (2014) 9346-9384. <https://doi.org/10.1021/cr400633s>.

[39] A. Mishra, B.S. Butola, Deposition of Ag doped TiO<sub>2</sub> on cotton fabric for wash durable UV protective and antibacterial properties at very low silver concentration, Cellulose. 24 (2017) 3555-3571. <https://doi.org/10.1007/s10570-017-1352-4>.

[40] D. Cheng, M. He, J. Ran, G. Cai, J. Wu, X. Wang, In situ reduction of TiO<sub>2</sub> nanoparticles on cotton fabrics through polydopamine templates for photocatalysis and UV protection, Cellulose. 25 (2018) 1413-1424. <https://doi.org/10.1007/s10570-017-1606-1>.

[41] S. Li, T. Zhu, J. Huang, Q. Guo, G. Chen, Y. Lai, Durable antibacterial and UV-protective Ag/TiO<sub>2</sub>@fabrics for sustainable biomedical application, Int. J. Nanomedicine. Volume 12 (2017) 2593-2606. <https://doi.org/10.2147/IJN.S132035>.

[42] Y. Liang, E. Pakdel, M. Zhang, L. Sun, X. Wang, Photoprotective properties of alpaca fiber melanin reinforced by rutile TiO<sub>2</sub> nanoparticles: A study on wool fabric, Polym. Degrad. Stab. 160 (2019) 80-88. <https://doi.org/10.1016/j.polymdegradstab.2018.12.006>.

- [43] R.D. Kale, T. Potdar, P. Kane, R. Singh, Nanocomposite polyester fabric based on graphene/titanium dioxide for conducting and UV protection functionality, *Graphene Technol.* 3 (2018) 35-46. <https://doi.org/10.1007/s41127-018-0021-1>.
- [44] M. Gorjanc, M. Šala, Durable antibacterial and UV protective properties of cellulose fabric functionalized with Ag/TiO<sub>2</sub> nanocomposite during dyeing with reactive dyes, *Cellulose.* 23 (2016) 2199-2209. <https://doi.org/10.1007/s10570-016-0945-7>.
- [45] M. Radeti, *Journal of Photochemistry and Photobiology C : Photochemistry Reviews* Functionalization of textile materials with TiO<sub>2</sub> nanoparticles Maja Radeti c, 16 (2013) 62-76.
- [46] M. Bragaglia, V. Cherubini, F. Nanni, PEEK -TiO<sub>2</sub> composites with enhanced UV resistance, *Compos. Sci. Technol.* 199 (2020) 108365. <https://doi.org/10.1016/j.compscitech.2020.108365>.
- [47] C. Li, Z. Li, X. Ren, Preparation and characterization of polyester fabrics coated with TiO<sub>2</sub>/Benzotriazole for UV protection, *Colloids Surfaces A Physicochem. Eng. Asp.* 577 (2019) 695-701. <https://doi.org/10.1016/j.colsurfa.2019.06.030>.
- [48] B. Seentrakoon, B. Junhasavasdikul, W. Chavasiri, Enhanced UV-protection and antibacterial properties of natural rubber/rutile-TiO<sub>2</sub> nanocomposites, *Polym. Degrad. Stab.* 98 (2013) 566-578. <https://doi.org/10.1016/j.polyimdeggradstab.2012.11.018>.
- [49] J.J. Reinoso, C.M.Á. Docio, V.Z. Ramírez, J.F.F. Lozano, Hierarchical nano ZnO-micro TiO<sub>2</sub> composites: High UV protection yield lowering photodegradation in sunscreens, *Ceram. Int.* 44 (2018) 2827-2834. <https://doi.org/10.1016/j.ceramint.2017.11.028>.
- [50] H. Sun, J. Weickert, H.C. Hesse, L. Schmidt-Mende, UV light protection through TiO<sub>2</sub> blocking layers for inverted organic solar cells, *Sol. Energy Mater. Sol. Cells.* 95 (2011) 3450-3454. <https://doi.org/10.1016/j.solmat.2011.08.004>.
- [51] N.K. Awad, S.L. Edwards, Y.S. Morsi, A review of TiO<sub>2</sub> NTs on Ti metal: Electrochemical synthesis, functionalization and potential use as bone implants, *Mater. Sci. Eng. C.* 76 (2017) 1401-1412. <https://doi.org/10.1016/j.msec.2017.02.150>.
- [52] V. Raj, M.S. Mumjitha, Fabrication of biopolymers reinforced TNT/HA coatings on Ti: Evaluation of its Corrosion resistance and Biocompatibility, *Electrochim. Acta.* 153 (2015) 1-11. <https://doi.org/10.1016/j.electacta.2014.10.055>.
- [53] A. Balamurugan, S. Kannan, S. Rajeswari, Evaluation of TiO<sub>2</sub> coatings obtained using the sol-gel technique on surgical grade type 316L stainless steel in simulated body fluid, *Mater. Lett.* 59 (2005) 3138-3143. <https://doi.org/10.1016/j.matlet.2005.05.036>.
- [54] E. Santos, N.K. Kuromoto, G.A. Soares, Mechanical properties of TiO<sub>2</sub> films used as biomaterials, *Mater. Chem. Phys.* 102 (2007) 92-97. <https://doi.org/10.1016/j.matchemphys.2006.11.010>.
- [55] M.A. Garcia-Lobato, A.I. Mtz-Enriquez, C.R. Garcia, M. Velazquez-Manzanares, F. Avalos-Belmontes, R. Ramos-Gonzalez, L.A. Garcia-Cerda, Corrosion resistance and in vitro bioactivity of dense and porous TiO<sub>2</sub> coatings deposited on 316L SS by spraying method, *Appl. Surf. Sci.* 484 (2019) 975-980. <https://doi.org/10.1016/j.apsusc.2019.04.108>.
- [56] X. Zhao, X. Liu, J. You, Z. Chen, C. Ding, Bioactivity and cytocompatibility of plasma-sprayed TiO<sub>2</sub> coating treated

by sulfuric acid treatment, Surf. Coatings Technol. 202 (2008) 3221-3226. <https://doi.org/10.1016/j.surfcoat.2007.11.026>.

[57] T. Peltola, M. Jokinen, H. Rahiala, M. Patsi, J. Heikkila, I. Kangasniemi, A. Yli-Urpo, Effect of aging time of sol on structure and in vitro calcium phosphate formation of sol-gel-derived TiO<sub>2</sub> films, J. Biomed. Mater. Res. 51 (2000) 200-208. [https://doi.org/10.1002/\(SICI\)1097-4636\(200008\)51:2<200::AID-JBM8>3.0.CO;2-Z](https://doi.org/10.1002/(SICI)1097-4636(200008)51:2<200::AID-JBM8>3.0.CO;2-Z).

[58] N. Matsumoto, K. Sato, K. Yoshida, K. Hashimoto, Y. Toda, Preparation and characterization of  $\beta$ -tricalcium phosphate co-doped with monovalent and divalent antibacterial metal ions, Acta Biomater. 5 (2009) 3157-3164. <https://doi.org/10.1016/j.actbio.2009.04.010>.

[59] X. He, G. Zhang, X. Wang, R. Hang, X. Huang, L. Qin, B. Tang, X. Zhang, Biocompatibility, corrosion resistance and antibacterial activity of TiO<sub>2</sub>/CuO coating on titanium, Ceram. Int. 43 (2017) 16185-16195. <https://doi.org/10.1016/j.ceramint.2017.08.196>.

[60] C.-M. Han, H.-E. Kim, Y.-H. Koh, Creation of hierarchical micro/nanoporous TiO<sub>2</sub> surface layer onto Ti implants for improved biocompatibility, Surf. Coatings Technol. 251 (2014) 226-231. <https://doi.org/10.1016/j.surfcoat.2014.04.030>.

[61] A.K.M. Kafi, G. Wu, A. Chen, A novel hydrogen peroxide biosensor based on the immobilization of horseradish peroxidase onto Au-modified titanium dioxide nanotube arrays, Biosens. Bioelectron. 24 (2008) 566-571. <https://doi.org/10.1016/j.bios.2008.06.004>.

[62] W.F. Oliveira, I.R.S. Arruda, G.M.M. Silva, G. Machado, L.C.B.B. Coelho, M.T.S. Correia, Functionalization of titanium dioxide

nanotubes with biomolecules for biomedical applications, Mater. Sci. Eng. C. 81 (2017) 597-606. <https://doi.org/10.1016/j.msec.2017.08.017>.

[63] Z. Zhang, Y. Xie, Z. Liu, F. Rong, Y. Wang, D. Fu, Covalently immobilized biosensor based on gold nanoparticles modified TiO<sub>2</sub> nanotube arrays, J. Electroanal. Chem. 650 (2011) 241-247. <https://doi.org/10.1016/j.jelechem.2010.10.016>.

[64] Q. Zhao, S. Tang, C. Fang, Y.-F. Tu, TiO<sub>2</sub> nanotubes decorated with gold nanoparticles for electrochemiluminescent biosensing of glycosylated hemoglobin, Anal. Chim. Acta. 936 (2016) 83-90. <https://doi.org/10.1016/j.aca.2016.07.015>.

[65] W. Zhang, J. Gu, C. Zhang, Y. Xie, X. Zheng, Preparation of TiO<sub>2</sub> coating by induction suspension plasma spraying for biomedical application, Surf. Coatings Technol. 358 (2019) 511-520. <https://doi.org/10.1016/j.surfcoat.2018.11.047>.

[66] S. Zhang, X. Liang, G.M. Gadd, Q. Zhao, Advanced titanium dioxide-polytetrafluorethylene (TiO<sub>2</sub>-PTFE) nanocomposite coatings on stainless steel surfaces with antibacterial and anti-corrosion properties, Appl. Surf. Sci. 490 (2019) 231-241. <https://doi.org/10.1016/j.apsusc.2019.06.070>.

[67] Z. Lu, M. Ren, H. Yin, A. Wang, C. Ge, Y. Zhang, L. Yu, T. Jiang, Preparation of nanosized anatase TiO<sub>2</sub>-coated kaolin composites and their pigmentary properties, Powder Technol. 196 (2009) 122-125. <https://doi.org/10.1016/j.powtec.2009.07.006>.

[68] I. Ali, M. Suhail, Z.A. Allothman, A. Alwarthan, Recent advances in syntheses, properties and applications of TiO<sub>2</sub> nanostructures, RSC Adv. 8 (2018) 30125-30147. <https://doi.org/10.1039/c8ra06517a>.

- [69] Oil and Colour Chemists' Association Australia, Titanium Dioxide Pigments, in: Surf. Coatings, Springer Netherlands, Dordrecht, 1983: pp. 305-312. [https://doi.org/10.1007/978-94-011-6940-0\\_26](https://doi.org/10.1007/978-94-011-6940-0_26).
- [70] Y. Liang, H. Ding, Mineral-TiO<sub>2</sub> composites: Preparation and application in papermaking, paints and plastics, *J. Alloys Compd.* 844 (2020) 156139. <https://doi.org/10.1016/j.jallcom.2020.156139>.
- [71] H. Zhou, M. Wang, H. Ding, G. Du, Preparation and Characterization of Barite/TiO<sub>2</sub> Composite Particles, *Adv. Mater. Sci. Eng.* 2015 (2015) 1-8. <https://doi.org/10.1155/2015/878594>.
- [72] Y. Chen, H. Yu, L. Yi, Y. Liu, L. Cao, K. Cao, Y. Liu, W. Zhao, T. Qi, Preparation of ground calcium carbonate-based TiO<sub>2</sub> pigment by a two-step coating method, *Powder Technol.* 325 (2018) 568-575. <https://doi.org/10.1016/j.powtec.2017.11.040>.
- [73] X. Zhao, J. Li, Y. Liu, Y. Zhang, J. Qu, T. Qi, Preparation and mechanism of TiO<sub>2</sub>-coated illite composite pigments, *Dye. Pigment.* 108 (2014) 84-92. <https://doi.org/10.1016/j.dyepig.2014.04.022>.
- [74] X.F. Hou, H. Ding, Y.X. Zheng, M.M. Wang, Preparation and characterisation of amorphous silica/anatase composite through mechanochemical method, *Mater. Res. Innov.* 17 (2013) 234-239. <https://doi.org/10.1179/1432891713Z.000000000222>.
- [75] S. Sun, H. Ding, H. Zhou, Preparation of TiO<sub>2</sub>-coated barite composite pigments by the hydrophobic aggregation method and their structure and properties, *Sci. Rep.* 7 (2017) 10083. <https://doi.org/10.1038/s41598-017-10620-7>.
- [76] X. Hou, Y. Zhang, H. Ding, P.K. Chu, Environmentally friendly wollastonite@TiO<sub>2</sub> composite particles prepared by a mechano-chemical method, *Particuology.* 40 (2018) 105-112. <https://doi.org/10.1016/j.partic.2017.10.010>.
- [77] S. Hazra, P.P. Bandyopadhyay, Scratch induced failure of plasma sprayed alumina based coatings, *Mater. Des.* 35 (2012) 243-250. <https://doi.org/10.1016/j.matdes.2011.09.014>.
- [78] S. Kar, P.P. Bandyopadhyay, S. Paul, Precision superabrasive grinding of plasma sprayed ceramic coatings, *Ceram. Int.* 42 (2016) 19302-19319. <https://doi.org/10.1016/j.ceramint.2016.09.100>.
- [79] P.P. Bandyopadhyay, S. Das, S. Madhusudan, A.B. Chattopadhyay, Wear and thermal fatigue characteristics of plasma-sprayed alumina coatings, *J. Mater. Sci. Lett.* 18 (1999) 727-729. <https://doi.org/10.1023/A:1006608715370>.
- [80] D. Mohanty, S. Kar, S. Paul, P.P. Bandyopadhyay, Carbon nanotube reinforced HVOF sprayed WC-Co coating, *Mater. Des.* 156 (2018) 340-350. <https://doi.org/10.1016/j.matdes.2018.06.054>.
- [81] D.S.R. Krishna, Y. Sun, Thermally oxidised rutile-TiO<sub>2</sub> coating on stainless steel for tribological properties and corrosion resistance enhancement, *Appl. Surf. Sci.* 252 (2005) 1107-1116. <https://doi.org/10.1016/j.apusc.2005.02.046>.
- [82] R.S. Lima, B.R. Marple, Thermal spray coatings engineered from nanostructured ceramic agglomerated powders for structural, thermal barrier and biomedical applications: A review, *J. Therm. Spray Technol.* 16 (2007) 40-63. <https://doi.org/10.1007/s11666-006-9010-7>.
- [83] M. Woydt, A. Skopp, I. Dörfel, K. Witke, Wear engineering oxides/

- antiwear oxides, *Wear*. 218 (1998) 84-95. <https://doi.org/10.1080/10402009908982185>.
- [84] Y. Sun, Tribological rutile-TiO<sub>2</sub> coating on aluminium alloy, *Appl. Surf. Sci.* 233 (2004) 328-335. <https://doi.org/10.1016/j.apsusc.2004.03.241>.
- [85] H. Dong, T. Bell, Enhanced wear resistance of titanium surfaces by a new thermal oxidation treatment, *Wear*. 238 (2000) 131-137. [https://doi.org/10.1016/S0043-1648\(99\)00359-2](https://doi.org/10.1016/S0043-1648(99)00359-2).
- [86] N. Dejang, A. Watcharapasorn, S. Wirojupatump, P. Niranatlumpong, S. Jiansirisomboon, Fabrication and properties of plasma-sprayed Al<sub>2</sub>O<sub>3</sub>/TiO<sub>2</sub> composite coatings: A role of nano-sized TiO<sub>2</sub> addition, *Surf. Coatings Technol.* 204 (2010) 1651-1657. <https://doi.org/10.1016/j.surfcoat.2009.10.052>.
- [87] P. Bagheri, M. Farzam, A.B. Mousavi, M. Hosseini, Ni-TiO<sub>2</sub> nanocomposite coating with high resistance to corrosion and wear, *Surf. Coatings Technol.* 204 (2010) 3804-3810. <https://doi.org/10.1016/j.surfcoat.2010.04.061>.
- [88] L.X. Ying, K. Wu, D.Y. Li, C.X. Wu, Z. Fu, TiO<sub>2</sub> Sol strengthened Cu-Sn-PTFE composite coatings with high homogeneity and superior resistance to wear, *Wear*. 426-427 (2019) 258-264. <https://doi.org/10.1016/j.wear.2019.01.031>.
- [89] N. nan Li, G. lu Li, H. dou Wang, J. jie Kang, T. shun Dong, H. jun Wang, Influence of TiO<sub>2</sub> content on the mechanical and tribological properties of Cr<sub>2</sub>O<sub>3</sub>-based coating, *Mater. Des.* 88 (2015) 906-914. <https://doi.org/10.1016/j.matdes.2015.09.085>.
- [90] P. Dinesh Babu, B. Prasannakumar, P. Marimuthu, R.K. Mishra, T. Ram Prabhu, Microstructure, wear and mechanical properties of plasma sprayed TiO<sub>2</sub> coating on Al-SiC metal matrix composite, *Arch. Civ. Mech. Eng.* 19 (2019) 756-767. <https://doi.org/10.1016/j.acme.2019.03.001>.
- [91] O. Çomaklı, M. Yazıcı, H. Kovacı, T. Yetim, A.F. Yetim, A. Çelik, Tribological and electrochemical properties of TiO<sub>2</sub> films produced on Cp-Ti by sol-gel and SILAR in bio-simulated environment, *Surf. Coatings Technol.* 352 (2018) 513-521. <https://doi.org/10.1016/j.surfcoat.2018.08.056>.
- [92] P.A. Dearnley, K.L. Dahm, H. Çimenoglu, The corrosion-wear behaviour of thermally oxidised CP-Ti and Ti-6Al-4V, *Wear*. 256 (2004) 469-479. [https://doi.org/10.1016/S0043-1648\(03\)00557-X](https://doi.org/10.1016/S0043-1648(03)00557-X).
- [93] R. Barkallah, R. Taktak, N. Guerhazi, K. Elleuch, J. bouaziz, Mechanical properties and wear behaviour of alumina/tricalcium phosphate/TiO<sub>2</sub> ceramics as coating for orthopedic implant, *Eng. Fract. Mech.* 241 (2021) 107399. <https://doi.org/10.1016/j.engfracmech.2020.107399>.
- [94] Z. Li, Z.J. Yao, A.A. Haidry, T. Plecenik, L.J. Xie, L.C. Sun, Q. Fatima, Resistive-type hydrogen gas sensor based on TiO<sub>2</sub>: A review, *Int. J. Hydrogen Energy.* 43 (2018) 21114-21132. <https://doi.org/10.1016/j.ijhydene.2018.09.051>.
- [95] Y.K. Jun, H.S. Kim, J.H. Lee, S.H. Hong, CO sensing performance in micro-arc oxidized TiO<sub>2</sub> films for air quality control, *Sensors Actuators, B Chem.* 120 (2006) 69-73. <https://doi.org/10.1016/j.snb.2006.01.045>.
- [96] B. Karunakaran, P. Uthirakumar, S.J. Chung, S. Velumani, E.K. Suh, TiO<sub>2</sub> thin film gas sensor for monitoring ammonia, *Mater. Charact.* 58 (2007) 680-684. <https://doi.org/10.1016/j.matchar.2006.11.007>.
- [97] N. Yamazoe, G. Sakai, K. Shimanoe, Oxide semiconductor gas sensors, *Catal.*

- Surv. from Asia. 7 (2003) 63-75. <https://doi.org/10.1023/A:1023436725457>.
- [98] V. Aroutiounian, Metal oxide hydrogen, oxygen, and carbon monoxide sensors for hydrogen setups and cells, *Int. J. Hydrogen Energy*. 32 (2007) 1145-1158. <https://doi.org/10.1016/j.ijhydene.2007.01.004>.
- [99] H. Tang, K. Prasad, R. Sanjinés, F. Lévy, TiO<sub>2</sub> anatase thin films as gas sensors, *Sensors Actuators, B Chem.* 26 (1995) 71-75. [https://doi.org/10.1016/0925-4005\(94\)01559-Z](https://doi.org/10.1016/0925-4005(94)01559-Z).
- [100] G.S. Devi, T. Hyodo, Y. Shimizu, M. Egashira, Synthesis of mesoporous TiO<sub>2</sub>-based powders and their gas-sensing properties, *Sensors Actuators, B Chem.* 87 (2002) 122-129. [https://doi.org/10.1016/S0925-4005\(02\)00228-9](https://doi.org/10.1016/S0925-4005(02)00228-9).
- [101] S. Yoo, S.A. Akbar, K.H. Sandhage, Nanocarving of TiO<sub>2</sub> (TiO<sub>2</sub>): A novel approach for fabricating chemical sensing platform, *Ceram. Int.* 30 (2004) 1121-1126. <https://doi.org/10.1016/j.ceramint.2003.12.085>.
- [102] Y.K. Jun, H.S. Kim, J.H. Lee, S.H. Hong, High H<sub>2</sub> sensing behavior of TiO<sub>2</sub> films formed by thermal oxidation, *Sensors Actuators, B Chem.* 107 (2005) 264-270. <https://doi.org/10.1016/j.snb.2004.10.010>.
- [103] J. Moon, M. Kemell, J. Kukkola, R. Punkkinen, H.P. Hedman, A. Suominen, E. Mäkilä, M. Tenho, A. Tuominen, H. Kim, Gas sensor using anodic TiO<sub>2</sub> thin film for monitoring hydrogen, *Procedia Eng.* 47 (2012) 791-794. <https://doi.org/10.1016/j.proeng.2012.09.266>.
- [104] J. Moon, H.P. Hedman, M. Kemell, A. Suominen, E. Mäkilä, H. Kim, A. Tuominen, R. Punkkinen, A study of monitoring hydrogen using mesoporous TiO<sub>2</sub> synthesized by anodization, *Sensors Actuators, B Chem.* 189 (2013) 246-250. <https://doi.org/10.1016/j.snb.2013.05.070>.
- [105] H. Liu, D. Ding, C. Ning, Z. Li, Wide-range hydrogen sensing with Nb-doped TiO<sub>2</sub> nanotubes, *Nanotechnology*. 23 (2012) 0-6. <https://doi.org/10.1088/0957-4484/23/1/015502>.
- [106] D. Gorman, A. Drewry, Y.L. Huang, C. Sames, The clinical toxicology of carbon monoxide, *Toxicology*. 187 (2003) 25-38. [https://doi.org/10.1016/S0300-483X\(03\)00005-2](https://doi.org/10.1016/S0300-483X(03)00005-2).
- [107] J.A. Raub, M. Mathieu-Nolf, N.B. Hampson, S.R. Thom, Carbon monoxide poisoning - A public health perspective, *Toxicology*. 145 (2000) 1-14. [https://doi.org/10.1016/S0300-483X\(99\)00217-6](https://doi.org/10.1016/S0300-483X(99)00217-6).
- [108] Y.J. Choi, Z. Seeley, A. Bandyopadhyay, S. Bose, S.A. Akbar, Aluminum-doped TiO<sub>2</sub> nano-powders for gas sensors, *Sensors Actuators, B Chem.* 124 (2007) 111-117. <https://doi.org/10.1016/j.snb.2006.12.005>.
- [109] N. Van Toan, C.M. Hung, N. Van Duy, N.D. Hoa, D.T.T. Le, N. Van Hieu, Bilayer SnO<sub>2</sub>-WO<sub>3</sub> nanofilms for enhanced NH<sub>3</sub> gas sensing performance, *Mater. Sci. Eng. B Solid-State Mater. Adv. Technol.* 224 (2017) 163-170. <https://doi.org/10.1016/j.mseb.2017.08.004>.
- [110] M. Gardon, O. Monereo, S. Dosta, G. Vescio, A. Cirera, J.M. Guilemany, New procedures for building-up the active layer of gas sensors on flexible polymers, *Surf. Coatings Technol.* 235 (2013) 848-852. <https://doi.org/10.1016/j.surfcoat.2013.09.011>.
- [111] P. Dhivya, A.K. Prasad, M. Sridharan, Nanostructured TiO<sub>2</sub> films: Enhanced NH<sub>3</sub> detection at room temperature, *Ceram. Int.* 40 (2014) 409-415. <https://doi.org/10.1016/j.ceramint.2013.06.016>.
- [112] U. Kirner, K.D. Schierbaum, W. Göpel, B. Leibold, N. Nicoloso, W.

Weppner, D. Fischer, W.F. Chu, Low and high temperature TiO<sub>2</sub> oxygen sensors, *Sensors Actuators B. Chem.* 1 (1990) 103-107. [https://doi.org/10.1016/0925-4005\(90\)80181-X](https://doi.org/10.1016/0925-4005(90)80181-X).

[113] L. Francioso, D.S. Presicce, A.M. Taurino, R. Rella, P. Siciliano, A. Ficarella, Automotive application of sol-gel TiO<sub>2</sub> thin film-based sensor for lambda measurement, *Sensors Actuators, B Chem.* 95 (2003) 66-72. [https://doi.org/10.1016/S0925-4005\(03\)00405-2](https://doi.org/10.1016/S0925-4005(03)00405-2).

[114] K. Moriya, T. Sako, Oxygen sensor monitoring a deterioration of a three-way catalyst in natural gas fueled engines, *Sensors Actuators, B Chem.* 73 (2001) 142-151. [https://doi.org/10.1016/S0925-4005\(00\)00683-3](https://doi.org/10.1016/S0925-4005(00)00683-3).

[115] L. Francioso, D.S. Presicce, M. Epifani, P. Siciliano, A. Ficarella, Response evaluation of TiO<sub>2</sub> sensor to flue gas on spark ignition engine and in controlled environment, *Sensors Actuators, B Chem.* 107 (2005) 563-571. <https://doi.org/10.1016/j.snb.2004.11.017>.

[116] J.H. Lee, Review on zirconia air-fuel ratio sensors for automotive applications, *J. Mater. Sci.* 38 (2003) 4247-4257. <https://doi.org/10.1023/A:1026366628297>.

[117] K. Naomasa Sunano, Akashi Naotatsu, Asahi Katsuta, Toshio Yoshida, *Gas Sensor And Method Of Producing The Same*, 4713646, 1987.